

# Behaviors of Free Bubble Nuclei in Inception of Sheet Cavitation

<sup>1</sup>Wakana Tsuru\*; <sup>1</sup>Satoshi Watanabe; <sup>1</sup>Shin-ichi Tsuda

<sup>1</sup>Kyushu University, Fukuoka, JAPAN

## Abstract

Inception of sheet cavitation is known to be a complex phenomenon depending upon the working flow conditions, especially on the boundary layer flow and the water quality. Because of this, it seems very difficult to simulate the sheet cavity inception by CFD using homogeneous cavitation model. In the present study, experimental observation of inception of sheet cavitation from a single free nucleus in a two-dimensional convergent-divergent nozzle is conducted under well degassed condition with few free nuclei. Then numerical simulation solving the equation of motion of bubble nuclei with Rayleigh-Plesset equation is conducted to see the effect of slippage of bubble nuclei from liquid flow on their trajectories. The flow field obtained by the single phase CFD is used as a background liquid flow. Finally, using the obtained bubble slip velocity, the spatial distribution of bubble nuclei density is estimated.

**Keywords:** sheet cavitation, inception, free bubble nuclei, slip velocity

## Introduction

Inception of sheet cavitation is known to be a complex phenomenon depending upon the working flow conditions. Many researches have been devoted to that in external flows around bodies such as hydrofoils and head forms since old times (for ex. [1]-[3]). Typically, when the laminar separation bubble is formed leading to the transition to turbulent flow, the sheet cavity forms not from the minimum pressure point but from the downstream separation bubble even though the pressure there is apparently larger than the minimum pressure [4]. This fact indicates that the behavior of free bubble nuclei is important for the formation of sheet cavity; it is necessary to have nuclei at the incipient point in sufficient time duration, but the nuclei seem to hardly approach to the minimum pressure point or hardly stay there sufficient time for their substantial growth.

The objective of this study is to understand nuclei behaviors in the process of sheet cavitation inception. The visual observation for free bubble nuclei near the throat wall of a two-dimensional convergent-divergent nozzle is conducted. Degassed water is used as working fluid. The general mechanism of attached sheet cavitation is briefly discussed. Then, numerical simulation tracking the motion of bubble nuclei in the liquid flow obtained by CFD is conducted to make clear the effect of slippage between bubble nuclei and liquid flow on their trajectories. The effect of the bubble growth is also investigated by solving Rayleigh-Plesset equation along with the equation of motion. Finally, the possible spatial distribution of bubble nuclei density is estimated by considering the conservation of bubble nuclei density with the above obtained bubble slip velocity.

## Experimental observation

Observations of sheet cavitation inception from free bubble nuclei is conducted in a two-dimensional convergent-divergent nozzle as shown in Figure 1 [5]. The size of test section is rather small, 20mm x 20mm, and the throat height is  $h=10\text{mm}$ . The maximum velocity at the nozzle throat is  $U_{throat}=10\text{m/s}$ , resulting in the maximum Reynolds number is about  $10^5$ . In order to observe the behavior of individual nucleus, it is important to reduce the nuclei density in the liquid. Therefore, multi-layered membrane filter with nominal pore diameter of  $1\mu\text{m}$  is installed in the test tunnel and the sufficient deaeration is carried out to reduce the dissolved gas content in water. The behaviors of nuclei are observed at the throat by a high-speed camera, from which the inception process is discussed.

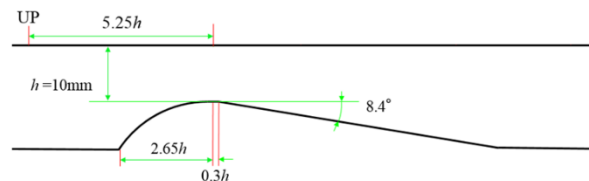


Figure 1 Dimensions of test nozzle. Flow direction is from left to right. Width is 20mm.

Figure 2 shows the typical inception process of sheet cavitation. Two series of snap shots are presented. Note that the two movies were taken separately, therefore the recorded bubbles are different ones, whereas these two movies give typical examples for sheet cavitation inception. From right-hand-side ones, it can be seen that a small bubble nucleus with the diameter less than 200 $\mu\text{m}$  in the top figure approaches to the nozzle wall, leading the sheet cavitation inception. From left-hand-side pictures, a large bubble attaches to the wall downstream of the throat, leaves the tail of itself on the wall and collapses downstream. In many cases of the observation results, it is confirmed that a free nucleus flowing near the wall at the throat region grows to a bubble. Then, the bubble attaches to the wall, and the tails of the bubble left on the wall develop to patch-like cavity, which can grow to sheet cavity. Although the static pressure takes the minimum at the throat, the locations of patch-like cavities and of leading edge of sheet cavity are slightly downstream.

From this movement of bubbles, it can be said that the free bubble nuclei tend to gather near the wall, as can be easily imagined by considering the light weight of bubbles with given pressure gradient, which would result in the larger number density of the bubble nuclei near the wall than in the free stream. However, the bubble nuclei itself does not grow to sheet cavitation, but would supply smaller portion onto the wall as a source of sheet cavitation.

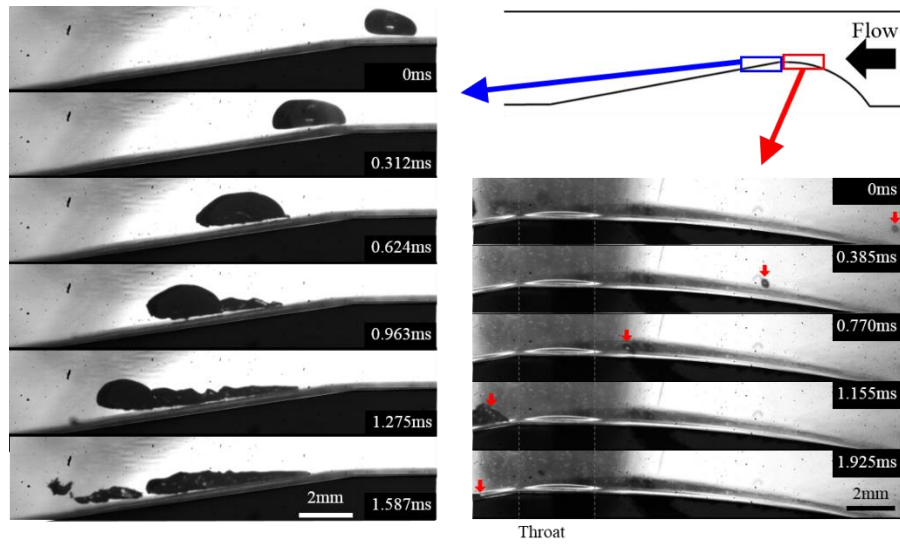


Figure 2 Typical sheet cavitation inception process from free bubble nuclei. Note that two series of movies (left and right) have been taken separately, tracking the different bubble nuclei.

### Numerical analysis

In order to analyze the motion of bubble nuclei, series of numerical simulation is conducted. Firstly, steady-state single-phase CFD is carried out to obtain the liquid flow field. The commercial CFD solver, ANSYS-CFX ver. 16.2 is used. Two-dimensional model is employed for simplicity. Shear Stress Transport model is employed as a turbulence model. The number of mesh nodes is around 105,000 and the normalized wall distance  $y^+$  is less than 0.1.

Once the liquid flow field is obtained, the bubble nucleus is tracked in Lagrange way by solving the following equation of motion of bubble nucleus.

$$\frac{4}{3}\pi r^3 \rho_b \frac{d\mathbf{v}_b}{dt} = \mathbf{F}_g + \mathbf{F}_p + \mathbf{F}_l + \mathbf{F}_d + \mathbf{F}_a + \mathbf{F}_r + \mathbf{F}_h + \mathbf{F}_w + \mathbf{F}_{other}$$

where  $r$  denotes the radius of bubble nucleus, and  $\rho_b$  and  $\mathbf{v}_b$  are density of gas and moving velocity of bubble nucleus respectively. The forces from  $\mathbf{F}_g$  to  $\mathbf{F}_{other}$  in RHS are the buoyancy force[6], the pressure gradient force[6], the lift force[7], the drag force[8], the added mass force[9][10], the force due to bubble growth[6], the history force, the force due to near wall[10] and the other forces respectively, which are determined from the corresponding literature. History force and other forces are neglected. The bubble tracking is carried out by time-integrating the above equation using the fourth order Runge-Kutta method until the bubble nucleus collides to the wall.

Along with solving the above equation of motion of bubble nucleus, Rayleigh-Plesset equation is solved for the growth of the bubble, which is expressed as

$$r \frac{d^2 r}{dt^2} + \frac{3}{2} \left( \frac{dr}{dt} \right)^2 = \frac{1}{\rho_l} \left( p_v - p + p_g - \frac{4\mu_l DR}{r} \frac{DR}{Dt} - \frac{2S}{r} \right)$$

where  $\rho_l$  is the density of liquid,  $p_v$  and  $p_g$  is the vapor pressure and the pressure of non-condensable gas,  $\mu_l$  is the viscosity of liquid and  $S$  is the surface tension. The pressure  $p$  is the local pressure which is taken from the result of single phase CFD. It is assumed that the non-condensable gas in the bubble nucleus obeys the isothermal law. Considering that the bubble is in a dynamic equilibrium condition at the inlet of numerical domain, the initial gas pressure  $p_{g0}$  can be determined with the given initial bubble radius  $r_0$  and the given upstream pressure  $p_0$  calculated from the assumed incipient cavitation number of  $\sigma = 2(p_0 - p_v)/\rho_l U_{throat}^2 = 0.9$ .

Figure 3(a) shows the examples of bubble trajectories with the initial bubble radius of  $r_0 = 50 \mu\text{m}$  (top) and  $5 \mu\text{m}$  (bottom). The throat velocity is  $U_{throat} = 10 \text{m/s}$ . Flow direction is from left to right. In this figure, the equation of bubble motion is only solved with the constant nucleus radius. The color of trajectories indicates the magnitude of slip velocity between liquid and bubble  $|\Delta v|$ . The grey colored lines show the liquid streamlines. From the figure, we can see the difference of bubble trajectories and liquid streamlines, which is more remarkable with the larger nucleus radius. Looking closely at the bottom corner of beginning of converging section (in dashed oval), so called ‘‘bubble screening effect’’ [2] due to the stagnant pressure can be recognized; the bubble nuclei go apart from the wall. Despite of this ‘‘screening effect,’’ the bubble nuclei approaches again to the wall near the throat as can be seen in the enlarged figure. This motion is also observed in the experiment as shown in the right-hand side snapshots of Figure 2. Finally, many of bubbles rapidly approach and collide to the wall.

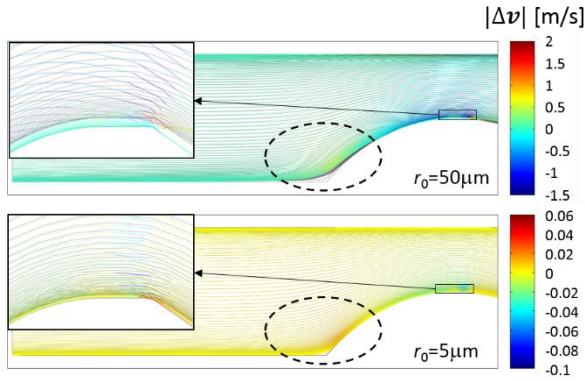


Figure 3(a) Trajectories of bubble nuclei with constant nuclei radius. The color indicates the magnitude of slip velocity.

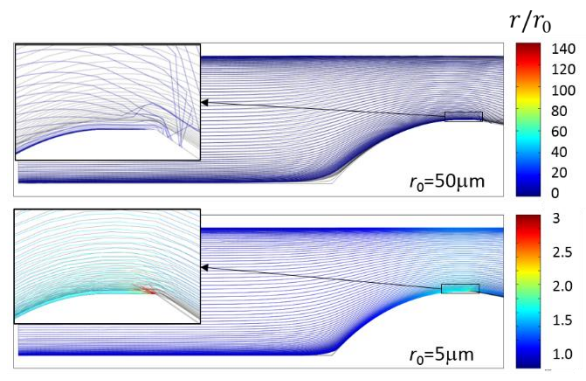


Figure 3(b) Trajectories of bubble nuclei with solving bubble growth equation. The color indicates the normalized bubble radius.

Figure 3(b) shows the examples of bubble trajectories with solving the bubble growth equation. The color of trajectories indicates the radius of bubble normalized by the initial bubble radius,  $r/r_0$ . By comparing this results with the previous one, it can be seen that the bubble trajectories are not very different in the regions far from the bottom nozzle wall. When the bubble nuclei approach to the wall roughly to the order of milli to sub-millimeter, the deviations is very remarkable, and it is seen that some bubble nuclei bounce violently. Since the spherical bubble has been assumed not only in Rayleigh-Plesset equation but also in the equation of motion, the obtained behaviors of bubbles very close to the wall seem to be inappropriate. Further modeling should be necessary to well reproduce the actual motion of bubble nuclei in near wall regions.

Although the bubble behaviors in near-wall region are somewhat strange, it seems to be still valuable to discuss the spatial distribution of the number density of bubbles due to the slippage between the liquid flow and the bubble velocity. By assuming the constant number density of bubble nuclei  $n_0$  upstream, the spatial distribution of bubble nuclei density  $n$  can be calculated from the bubble and liquid velocity distributions obtained above. Neglecting the bubble growth for simplicity, the following equation is obtained from the conversation law of number density of bubble nuclei.

$$\frac{D_g}{Dt} \left( \frac{n}{n_0} \right) = -\frac{n}{n_0} \nabla \cdot \mathbf{v}_g \quad \text{or} \quad \frac{D_g}{Dt} \ln \left( \frac{n}{n_0} \right) = -\nabla \cdot \mathbf{v}_g$$

where  $D_g/Dt$  is the time derivative along with bubble motion. After time-integrating this equation along the bubble trajectory like in Figure 3(a), and interpolating them to the mesh used in CFD, the distribution of number density is obtained as shown in Figure 4.

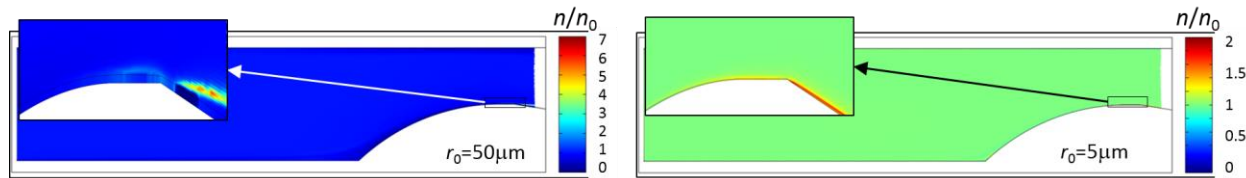


Figure 4 Calculated spatial distribution of nuclei number density for the nuclei radius of  $r_0=50\mu\text{m}$  (left) and  $r_0=5\mu\text{m}$  (right).

Since the near-wall motions of bubble nuclei are not well solved as mentioned before, the number densities near the wall (within wall distance less than  $2r_0$ ) have been calculated by the extrapolation considering its normal gradient to the wall is zero. The accumulation of the bubble nuclei near the wall can be seen from upstream of the nozzle throat in the case with  $r_0=5\mu\text{m}$  (right). On the other hand, in the case with  $r_0=50\mu\text{m}$  (left), the largest number density can be seen downstream of the nozzle throat and a little far from the wall. However, more accurate treatment of bubble motions are necessary for further discussion on the bubble density distribution and the sheet cavitation inception.

## Conclusion

In the present study, the visual observation of sheet cavitation inception from a free bubble nuclei in a two-dimensional convergent-divergent nozzle is conducted to obtain some general overview of inception mechanism of sheet cavitation. In many cases, it is observed that bubble nuclei in free stream approach to the wall and some portion is attached and left on the wall, resulting in a patch-like cavity as a source of sheet cavitation. Numerical simulation of bubble motion is conducted, and it is found that the effect of slip velocity of bubble nuclei to liquid flow is significant and the trajectories of bubble nuclei is similar to those observed in experiments. The number density of bubble nuclei is found to be larger near the throat due to the slippage effect, whereas the further study is needed especially on establishment of more sophisticated model for bubble nuclei moving near the wall.

This work was partly supported by JSPS KAKENHI Grant Number JP17J04154. Numerical simulation was mainly carried out using the computer facilities at Research Institute for Information Technology, Kyushu University.

## References

- [1] Knapp, R. T., Hollander, A. (1948). *Laboratory investigations of the mechanism of cavitation*. ASME J. Fluids Eng. 70, pp. 419-433.
- [2] Kodama, Y., Take, N., Tamiya, S., Kato, H. (1981). *The effect of nuclei on the inception of bubble and sheet cavitation on axisymmetric bodies*. ASME J. Fluids Eng. 103, pp. 557-563.
- [3] Rijsbergen, M. (2016). *A Review of Sheet Cavitation Inception Mechanisms*, Proc. ISROMAC2016. 356.
- [4] Arakeri, H., Acosta, A. J. (1976). *Cavitation inception observations on axisymmetric bodies at supercritical Reynolds numbers*. J. Ship Research. 20, pp. 40-50.
- [5] Tsuru, W., Konishi, T., Watanabe, S., Tsuda, S. (2017). *Observation of inception of sheet cavitation from free nuclei*. J. Thermal Science. 26(3), pp. 223-228.
- [6] Shams, E., Finn, J., Apte, S. V. (2011). *A numerical scheme for Euler-Lagrange simulation of bubbly flows in complex systems*. Int. J. Numerical Method of Fluids. 67, pp. 1865-1898.
- [7] Antal, S. P., Lahey Jr, R. T., Flaherty, J. E. (1991). *Analysis of phase distribution in fully developed laminar bubbly two-phase flow*. Int. J. Multiphase Flow. 17(5), pp. 635-52.
- [8] Tomiyama, A., Sou, A., Minagawa, H., Sakaguchi, T. (1991). *Numerical analysis of a single bubble with VOF method*. Trans. JSME, Ser. B (in Japanese). 57, pp. 2167-2173.
- [9] Brennen, C. E. (1995). *Cavitation and bubble dynamics*. Oxford University Press.
- [10] Sanada, T., Sato, A., Shirota, M., Watanabe, M. (2009). *Motion and coalescence of a pair of bubbles rising side by side*. Chemical Engineering Science. 64(11), pp. 2659-2671.